Engineering Structures 279 (2023) 115616

Contents lists available at ScienceDirect

Engineering Structures

journal homepage: www.elsevier.com/locate/engstruct

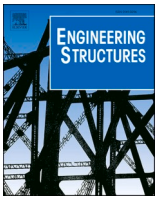

Long-term health monitoring of concrete and steel bridges under large and missing data by unsupervised meta learning

Alireza Entezami [a,*], Hassan Sarmadi [b,c], Bahareh Behkamal [a]

[a] Department of Civil and Environmental Engineering, Politecnico di Milano, Milan, Italy
[b] Department of Civil Engineering, Faculty of Engineering, Ferdowsi University of Mashhad, Mashhad, Iran
[c] Head of Research and Development, IPESFP Company, Mashhad, Iran

ARTICLE INFO

Keywords:
Structural health monitoring
Environmental variability
Freezing air temperature
Large data
Modal frequency
Unsupervised learning
Meta-learning

ABSTRACT

Long-term monitoring brings an important benefit for health monitoring of civil structures due to covering all possible unpredictable variations in measured vibration data and providing relatively adequate training samples for unsupervised learning algorithms. Despite such merits, this process may encounter large data with missing values and also yield erroneous results caused by severe environmental changes, particularly those emerge as sharp increases in modal frequencies during freezing weather. To address these challenges, this article proposes a novel unsupervised meta-learning method that entails four steps of an initial data analysis, data segmentation, subspace searching by a novel approach called nearest cluster selection, and anomaly detection. The first step intends to initially analyze measured data/features for cleaning missing samples. Next, the second step exploits spectral clustering to divide clean data into some segments. In the third step, the proposed nearest cluster selection is utilized to measure dissimilarities between the segments by a distance metric and select a cluster with the minimum distance as the representative of the main segment. Finally, a locally robust Mahalanobis-squared distance is applied by merging the concepts of robust statistics and local metric learning for online anomaly detection. The key innovations of this research contain developing a new unsupervised learning strategy alongside a locally robust distance and proposing the idea of nearest cluster selection. Long-term modal frequencies of full-scale concrete and steel bridges are used to verify the proposed method. Results demonstrate that this method succeeds in mitigating severe environmental effects and accurately detecting damage.

1. Introduction

Civil structures are important and basic systems of any society due to their dependency on economic and social life. These structures are subjected to various excitation sources of live loads, natural and man-made hazards. On the other hand, most of the civil structures were designed and built several decades ago with outdated design codes and construction techniques. Under such circumstances, material deterioration and aging are critical factors that jeopardize structural safety and integrity. To prevent any catastrophic events such as failure and collapse due to the occurrence and growth of damage, structural health monitoring (SHM) has become an essential necessity in civil engineering communities for bridges [1], buildings [2], dams [3], etc. The main objective of an SHM program is to design a systematic framework for assessing the current state of a civil structure in terms of early damage detection, damage localization, and damage severity estimation by measuring different structural responses.

Because of recent progress in sensing technologies alongside data acquisition and transmission systems, it is possible to equip civil structures with various sensors [4,5]. On this basis, one can extract meaningful features directly relevant to inherent physical properties, particularly structural stiffness, from measured structural responses. Natural frequencies are among popular and suitable features for long-term SHM, which is often conducted within one or several years [6–8], and early damage detection due to their simple identification via different modal analysis techniques [9] and the minimum requirement for sensor deployment and placement. However, such dynamic features are profoundly influenced by unpredictable environmental (e.g., temperature, moisture, humidity, wind) and operational (e.g., excessive live loads, massive traffic) changes. The demanding issue is that both environmental and/or operational (E/O) conditions can vary the intrinsic physical properties and structural responses similar to damage. In this

* Corresponding author.
E-mail address: alireza.entezami@polimi.it (A. Entezami).

https://doi.org/10.1016/j.engstruct.2023.115616
Received 15 September 2022; Received in revised form 8 December 2022; Accepted 8 January 2023

regard, Larsson et al. [8] studied long-term analysis of environmental changes in modal data of a hybrid timber-concrete building and concluded that the natural frequencies are significantly sensitive to seasonal temperature fluctuations. Zhou and Sun [10] evaluated the effects of the E/O changes on a sea-crossing bridge and deduced that temperature and traffic loads are the critical factors for structural changes. Zonno et al. [11] analyzed long and short-term influences of temperature and humidity on an adobe church building and concluded that humidity changes have stronger impacts on the structural properties in long-term monitoring, while both temperature and humidity are more important for short-term monitoring. Martin et al. [12] conducted dynamic monitoring on a stadium suspension roof under temperature and wind effects and deduced that such environmental conditions, especially temperature variability, can make the most changes in the roof natural frequencies.

On the other hand, the other important point regarding the E/O variability is sudden changes in vibration data, particularly natural frequencies, during normal operations. In some slender structures (e.g., bridges or masonry bell towers), the temperature variability in cold days (i.e., when the temperature is often below 0 °C), the natural frequencies exhibit sharp increases. An interesting note is that this phenomenon is independent of the type of structural material so that it was observed in different civil structures such as a concrete box-girder bridge [13], an arch steel bridge [14], and masonry buildings [6]. Under such circumstances, it is possible to receive an incorrect alarm regarding the occurrence of damage, while the structure operates normally. This situation refers to a false alarm or false positive error that leads to economic losses alongside time-consuming and redundant inspection efforts. On the other hand, the severity of the E/O variability can be much larger than structural damage, particularly minor damage, in such a way that one cannot detect damage appropriately. This situation results in a false negative error that threatens human safety and causes injuries or even deaths in case of the occurrence of failure or collapse. Thus, it is indispensable to capture all possible E/O changes in continuous long-term monitoring and remove their influences on structural responses and features to perform a reliable SHM process [15].

1.1. Background of machine learning-aided SHM

The important issue in long-term SHM is concerned with the main methodology for this process. Recently, artificial intelligence brings a great opportunity to simulate the human brain based on various machine learning (ML) algorithms [16,17]. Generally, a ML algorithm aims to develop a computational model using training data in terms of supervised and unsupervised learning classes. In the context of SHM, a fully labeled set suitable for supervised learning contains the damage-sensitive features of both undamaged and damaged conditions, while unlabeled data used in unsupervised learning consists of the features of the only undamaged condition. When there is no sufficient information about the damaged state during the training phase (i.e., unlabeled data is only available), unsupervised learing is a proper choice.

A prominent demand in unsupervised learning-based SHM is related to accurate decision-making via large and missing data (features) in long-term monitoring under severe E/O changes. Generally, long-term SHM through unlabeled data in the presence of unpredictable variability conditions is a complex process. This is because such a process can produce large data with different types of outliers caused by the E/O conditions and also loss some important information (missing data) due to sensor and measurement instrument malfunctions, poor installation, storage and transmission system downtime, harsh working environment, etc. [18]. Therefore, it is essential to develop a robust unsupervised learning model that should not only overcome the serious E/O effects but also suit under large and missing data. Regarding ML-aided methods for SHM under the E/O changes, Sarmadi and Yuen [19] proposed an unsupervised kernel-based method under the concept of kernel null space, which could significantly eliminate the variations in natural frequencies caused by the E/O conditions and provide discriminative anomaly scores for long-term SHM. Giglioni et al. [20] compared some state-of-the-art unsupervised learners developed from principal component analysis (PCA) in global and local versions and Gaussian mixture model (GMM) for removing the influences of environmental variability in long-term SHM of a concrete bridge and a masonry building. In their research, the local PCA demonstrated the best performance. Mousavi et al. [21] studied the influence of temperature on natural frequencies by exploiting some state-of-the-art supervised regression models and extracting their prediction errors for damage detection. Daneshvar and Sarmadi [22] proposed a novel anomaly detector based on the concepts of unsupervised feature selection and local density analysis for SHM under different E/O variability in short- and long-term monitoring. Their anomaly detector could not only mitigate the E/O effects but also yield high damage detectability. Rogers et al. [23] developed an innovative Bayesian non-parametric clustering algorithm based on Dirichlet process mixture models in terms of semi-supervised learning for SHM under severe E/O changes and the availability of limited training data. Sarmadi and Yuen [24] proposed a novel probabilistic unsupervised learning method via the concepts of extreme value theory, mixture quantile modeling, and unsupervised nearest neighbor searching for damage detection in concrete bridges with statistical and dynamic features. They concluded that the unsupervised nearest neighbor searching is an effective tool for removing the E/O effects. Entezami et al. [25] introduced the theory of empirical learning to SHM by proposing an innovative unsupervised learner in a non-parametric fashion for bridge damage identification under severe environmental variability. An important note about the aforementioned techniques is that those disregard missing data and continue the SHM process by the remaining data/features.

As an alternative, the second methodology brings the possibility of recovering or predicting missing data and performs long-term SHM via original and recovered data/features. In this regard, Ma et al. [26] suggested a probabilistic PCA model for recovering missing samples of a feature dataset comprising static stress data and then considered Q-statistic and T^2-statistic of this model as anomaly detectors. Under multiple operational conditions of a stadium with a retractable roof and missing data, Ma et al. [27] developed a mixture of the probabilistic PCA for retrieving missing points and implementing damage detection and localization with the aid of three anomaly detectors (i.e., the Q-statistic and T^2-statistic along with a residual statistic). Xu et al. [28] took advantage of a robust PCA model to predict missing data by adding virtual random errors to the locations of the missing entities and then detect damage under such data prediction. Xu et al. [29] proposed a low-rank matrix approximation method to impute missing data and then considered a cointegration analysis to remove the E/O influences from modal frequencies for long-term SHM. Despite the applicability of the second methodology, it may need additional techniques for missing data recovery and also more computational time compared to the first methodology, which is only based on removing missing data. Thus, this article intends to take advantage of the first methodology.

On the other hand, since no labeled data is available in unsupervised learning-based SHM, the main task is to measure the dissimilarity between at least two feature sets regarding two different structural conditions in an effort to detect and localize damage [42,46]. In most cases, the use of a standard distance measure by considering the whole data (e.g., the Mahalanobis distance by estimating the mean vector and covariance matrix of the entire training data) is prevalent. However, this global learning approach encounters two major limitations. First, it may ignore some important properties available in unlabeled data. Second, the consideration of the whole data is not a robust way for anomaly detection. This is because outliers, noise, and E/O conditions may affect the statistical properties of the whole data (e.g., the mean and standard deviation) and cause erroneous outputs [30]. This issue is directly related to the problem of damage detectability in SHM [31]. In other words, a robust unsupervised learner is one that can provide

discriminative damage indices for decision-making and differentiate the possibly damaged condition from the normal one.

To deal with the problem stemming from the utilization of the whole large data in ML, local learning is an effective solution. This technique takes advantage of some new concepts such as subspace searching [32] and local distance learning [33]. The idea behind the local distance learning emanates from the development of a distance function for a specific problem (i.e., the mitigation of the negative effects of the E/O conditions) by using local subsets of the whole data. The major advantages of this technique contain the preparation of more rich data compared to global learning and the resilient to outliers due to utilizing the local information [34]. On the other hand, the theory of subspace searching relies upon analyzing different subsets of features and extracting the most useful feature samples from such local information while keeping original contents of the whole data. Although this technique resembles feature selection, it is implemented locally.

Finally, the other major challenge in unsupervised SHM is to apply a single learner (model) for a problem. Although this strategy is plausible and promising, it is possible to obtain better results by leveraging meta-learning. From the ML perspective, meta-learning is an advanced method that intends to develop a new hybrid model by using the outputs of other single machine learners previously learned from data [35]. Simply speaking, if a single model learns how to appropriately use information for a task (e.g., classification, prediction, clustering, anomaly detection), a meta-learner learns how to best utilize the outputs of that single learner for performing the same learning task or provide new (better) outputs. For this purpose, it suffices to learn from prior information or outputs of the previous learners in a systematic data-driven manner. On this basis, one initially needs to collect meta-data or meta-features that describe prior learning tasks and previously learned models. Subsequently, it is necessary to learn from meta-features based on the prior learning process to extract and transfer new knowledge (features) that can yield better performance [35]. As a meta-learner can be developed by combining some single learners in a hybrid fashion, the great advantage of meta-learning is to improve the overall performance of a single learner. For the long-term monitoring, this technique can bring some benefits such as addressing the challenges of this kind of monitoring scheme (e.g., the E/O effects) and achieving reliable results of SHM with the minimum rates of decision-making errors.

1.2. Motivations

This article proposes an innovative unsupervised meta-learing (UML) method for long-term monitoring of civil structures, especially bridges, in the presence of large and missing data (features) influenced by profound environmental variability during freezing weather. In essence, this method develops a hybrid unsupervised learner that entails four main steps of an initial data analysis, data segmentation through spectral clustering, a subspace search algorithm by a new idea called nearest cluster selection (NCS), and anomaly detection via a locally robust Mahalanobis-squared distance (LRMSD) based on the concepts of local distance metric learning and robust statistics. In order to alleviate the limitation of the existence of missing data, the initial data analysis in the first step seeks in training and test datasets to remove any missing value and provide clean features for the next steps. Having considered the whole clean training data, the second step exploits the spectral clustering to divide the training features into some segments/clusters and provide the initial local information/subsets. This process refers to the first step of meta-learning, in which case the outputs of clustering are indicative of meta-features. Utilizing the idea of the subspace searching based on the proposed NCS algorithm, the third step makes an attempt to extract the most useful features within a cluster from the initial local subsets. For this purpose, a cumulative Mahalanobis-squared distance (CMSD) is applied to perform distance calculations among these subsets and find a segment/cluster with the minimum distance value, which is the representative set with the most useful information. Eventually, the proposed LRMSD measure is employed to compute anomaly indicators (scores) for damage detection. Large sets of long-term modal frequencies of two different bridges (i.e., a concrete box-girder bridge and a steel arch bridge) are incorporated to validate the effectiveness and reliability of the proposed method alongside several comparisons. Results demonstrate that this method is able to detect damage and mitigate the serious influences of environmental variations.

2. Contributions

The main contributions of this research can be summarized as: (i) developing a novel UML framework for long-term SHM under severe E/O changes, (ii) proposing the idea of NCS, and (iii) applying a locally robust multivariate distance metric for anomaly detection. In relation to the second contribution, it should be clarified that the key novel part of the NCS is to select the representative of an original cluster and use this representative and its feature samples in a learning process rather than the information (features) of the original cluster. The other novelty of this approach is to implement a locally unsupervised feature selection. Compared to most of the unsupervised feature selection techniques, which consider the whole data and choose a part of such data, the proposed NCS approach conducts a different feature selection procedure in a local manner. Regarding the third contribution, the main innovation of the LRMSD relates to its general framework that originates from the ideas of local learning and robust statistics for long-term health monitoring of civil structures. Even though Sarmadi et al. [34] developed a locally distance measure based on the MSD, this article enhances their work by merging the concepts of robust statistics and local distance learning. More precisely, they exploited a locally centered covariance estimator for developing their local distance measure, while this article exploits a robust covariance estimator in conjunction with local information from the previous steps of the proposed UML method for deriving the LRMSD metric.

3. Proposed method

3.1. Initial data analysis

ML methods may not operate properly in the presence of missing data in both training and test datasets. On the other hand, it may be difficult to predict such data. In this case, an initial data analysis is needed to explore available data and discard any missing samples before learning any ML model. In the proposed method, this analysis is carried out in two stages of offline learning and online anomaly detection in the training and inspection stages, respectively. Throughout the training period, one supposes that there are adequate training samples, which can capture all possible E/O conditions and obtain large data. Accordingly, these points are collected into a matrix whose rows and columns represent the feature values (e.g., the modal frequencies of all measured modes) and feature samples (e.g., the number of measurements). On this basis, one attempts to seek in the feature samples (i.e., the column vectors of the training matrix) and remove any feature vector with only one missing value. Fig. 1(a) shows the graphical representation of the initial data analysis in the training phase.

For the inspection phase, it is assumed that there is only one test sample at each time to perform online anomaly detection. Therefore, the initial data analysis should be implemented on a feature vector. If this vector contains any missing value, one should ignore it. One of the advantages of implementing online anomaly detection in the inspection phase is that both data measurement and initial analysis can be conducted simultaneously. Hence, if a test sample should be eliminated, one can repeat the measurement process for providing new test data. Fig. 1 (b) illustrates the procedure of the initial data analysis in the inspection phase. Note that the word “sample” refers to a feature vector. In this article, a sample is a vector of the natural frequencies obtained from some modes. For example, the test vector in Fig. 1(b) is a sample.

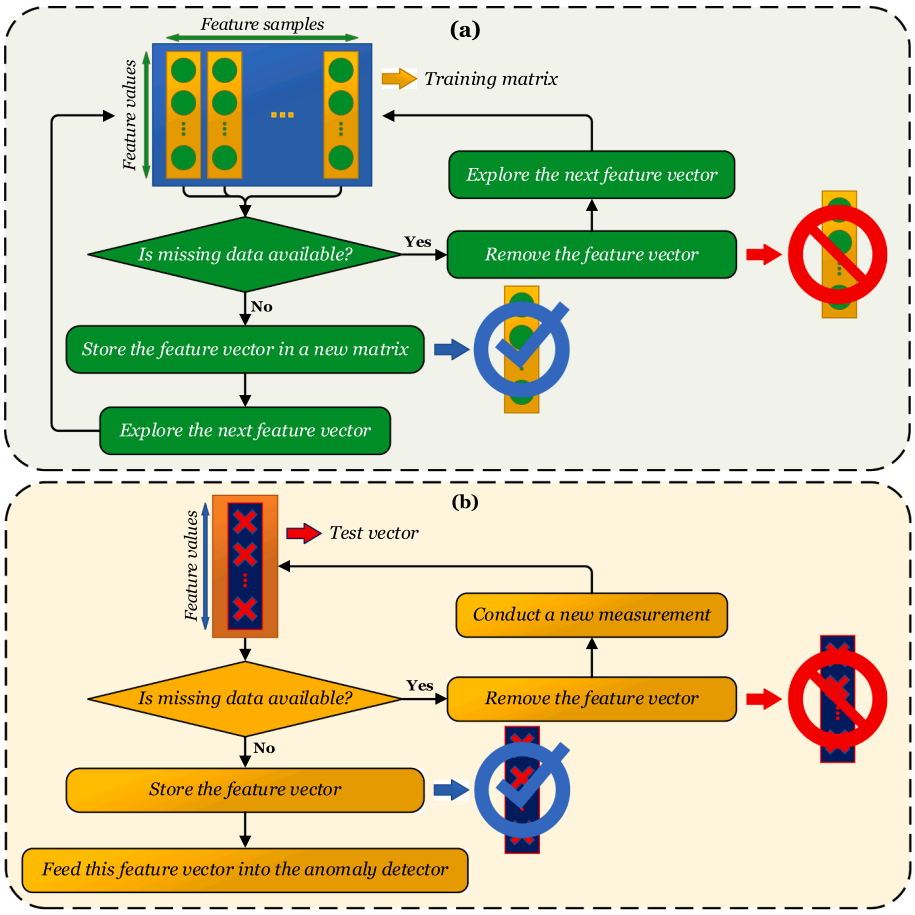

Fig. 1. The graphical representation of the initial data analysis for discarding missing values: (a) the training phase, (b) the inspection phase.

3.2. Data segmentation by spectral clustering

Spectral clustering is a graph-based data segmentation technique under the graph theory for finding some arbitrary shaped clusters in sampling data [36]. This technique is based on representing the data in a low dimension so that clusters are more widely separated. To implement the spectral clustering, one needs to determine its requirements; that is, an undirected graph as well as similarity and Laplacian matrices. The undirected graph models the local neighborhood relationships between data points. The nodes in the graph are indicative of these points and the undirected edges build their connections. The similarity matrix describes the similarity graph that consists of pairwise distance quantities between the connected nodes in the graph. Eventually, the Laplacian matrix is a set for representing the similarity graph.

Suppose that $\mathbf{X}\in\mathbb{R}^{p\times n}$ is a training matrix containing n natural frequencies obtained from p modes. The first step of the spectral clustering is to determine the similarity matrix by calculating the pairwise distances between n feature samples (i.e., natural frequencies) of $\mathbf{X}$ as follows:

$$S_{ij}=\exp\left(\left(\frac{d_{ij}}{\sigma}\right)^2\right) \tag{1}$$

where S_{ij} stands for the i^{th} row and the j^{th} column of the similarity matrix $\mathbf{S}\in\mathbb{R}^{n\times n}$; d_{ij} is the distance between the i^{th} and j^{th} samples; and σ denotes the kernel scale, which corresponds to one in this article. In the following, the Laplacian matrix can be determined by using one of the following equations:

$$\mathbf{L}_u=\mathbf{D}_g-\mathbf{S} \tag{2}$$

$$\mathbf{L}_n=\mathbf{D}_g{}^{-1}\mathbf{L}_u \tag{3}$$

$$\mathbf{L}_s=\mathbf{D}_g{}^{-\frac{1}{2}}\mathbf{L}_u\mathbf{D}_g{}^{-\frac{1}{2}} \tag{4}$$

where $\mathbf{L}_u$, $\mathbf{L}_n$, and $\mathbf{L}_s$ represent the unnormalized, normalized, and symmetric normalized Laplacian matrices, respectively. In Eqs. (2)-(4), $\mathbf{D}_g\in\mathbb{R}^{n\times n}$ refers to the degree matrix derived from $\mathbf{S}$ whose i^{th} diagonal element is expressed by $D_g(i,i)=\sum_{j=1}^{n}S_{i,j}$. In Eq. (3), the normalized Laplacian matrix is determined by solving the generalized eigenvalue problem $\mathbf{L}_u\mathbf{v}=\lambda\mathbf{D}_g\mathbf{v}$, where $\mathbf{v}$ is a column eigenvector of length n, and λ is an eigenvalue. Using the Laplacian matrix and considering the number of clusters c, the spectral clustering makes the matrix $\mathbf{V}\in\mathbb{R}^{n\times c}$ containing c eigenvectors $\{\mathbf{v}_1,\ldots,\mathbf{v}_c\}$ obtained from the c smallest eigenvalues of the Laplacian matrix. Each n-dimensional row of the matrix $\mathbf{V}$ can be clustered by one of the partition-based clustering algorithms (e.g., k-means or k-medoids clustering[1]). Eventually, the n feature samples of $\mathbf{X}$ are allocated to the same clusters as their corresponding rows in $\mathbf{V}$ and get the labels $\{1,\ldots,c\}$ leading to obtaining c clusters/partitions $\{\mathbf{C}_1,\ldots,\mathbf{C}_c\}$.

To determine the number of clusters c, which is the only hyperparameter of the spectral clustering, this article utilizes the gap statistic proposed by Tibshirani et al. [37]. This technique compares the total intra-cluster variations in different cluster numbers with their expected values under null reference distribution (i.e., a distribution with no obvious clustering) of data. The output of this process is the value of the gap statistic (G). For the k^{th} cluster number (trial), this value is given by:

[1] The variable k in these clustering techniques refers to the number of clusters.

$G_k = E(\log W_k) - \log W_k$(5).

where E denotes the expectation value and W_k is a measure of the compactness of the spectral clustering based on the within-cluster-sum-of-squared error in the k^{th} cluster, which is expressed as follows:

$$W_k = \sum_{i=1}^{k} \frac{1}{2r_i}\rho_i \tag{6}$$

where r_i denotes the number of samples (i.e., column vectors) of the i^{th} cluster $\mathbf{C}_i \in \mathbb{R}^{p\times r_i}$ and ρ_i is the sum of the pairwise distances of all samples in this cluster. Under different cluster numbers (trials), the optimal choice is one that satisfies the following condition:

$$G_k \geq G_{k+1} - \delta_{k+1} \tag{7}$$

where δ is the one-standard-error of W with respect to the reference data for each cluster. It is worth remarking that $E(\log W_k)$ is determined by Monte Carlo sampling from a reference distribution, and $\log W_k$ is computed from the sample data.

3.3. Subspace searching by nearest cluster selection

Generally, most of the cluster-based anomaly detection methods consider all clusters to determine anomaly scores with the aid of a detector model (e.g., MSD) and select the minimum score value as the final choice. This article proposes the idea of NCS originated from the subspace searching, which neither transforms the original feature space nor reduces the dimension of data [32]. On this basis, the NCS approach aims to find the nearest cluster/subset of each initial segment obtained from the data segmentation step and use it as the representative of the original initial segment for anomaly detection. For simplicity, Fig. 2 shows the graphical representation of this approach.

Given the clusters/segments $\{\mathbf{C}_1,\ldots,\mathbf{C}_c\}$ from the data segmentation process (i.e., meta-features), the key step of the NCS is to perform distance calculations. For this purpose, one of the initial segments is chosen as reference and the remaining clusters as targets. The distance calculation is based on computing the dissimilarity between the reference and target clusters. In the next step, the target subset with the minimum distance (i.e., the nearest cluster) is selected as the representative of the reference cluster. Let $\mathbf{C}_i$ and $\{\mathbf{C}_1,\ldots,\mathbf{C}_{i-1},\mathbf{C}_{i+1},\ldots,\mathbf{C}_c\}$ denote the reference and target clusters, respectively. Since all of them are multivariate, the distance calculation can be carried out by any multivariate statistical

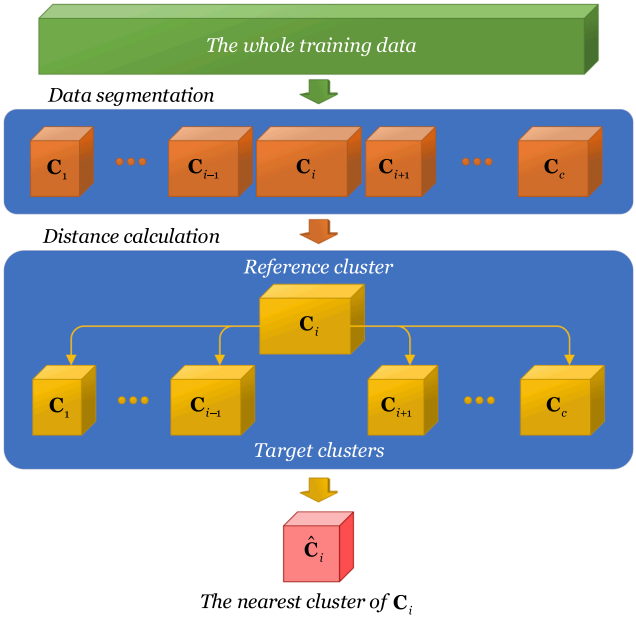

Fig. 2. The graphical representation of the proposed NCS approach.

distance such as the proposed CMSD. For example, the distance calculation between the i^{th} and $(i\text{-}1)^{\text{th}}$ clusters can be expressed as follows:

$$D(\mathbf{C}_i, \mathbf{C}_{i-1}) = \sum_{j=1}^{r_i} \left(\left(\mathbf{c}_{i-1}^{(j)} - \mathbf{m}_i \right)^T \mathbf{H}_i^{-1} \left(\mathbf{c}_{i-1}^{(j)} - \mathbf{m}_i \right) \right) \tag{8}$$

where $\mathbf{m}_i \in \mathbb{R}^p$ and $\mathbf{H}_i \in \mathbb{R}^{p\times p}$ denote the mean vector and standard covariance matrix of the i^{th} (reference) cluster; $\mathbf{c}_{i-1}^{(j)} \in \mathbb{R}^p$ is the j^{th} row vector of the $(i\text{-}1)^{\text{th}}$ target cluster. Moreover, $D(\mathbf{C}_i,\mathbf{C}_{i-1})$ stands for the CMSD value between $\mathbf{C}_i$ and $\mathbf{C}_{i-1}$. Accordingly, the nearest cluster $\widehat{\mathbf{C}}_i$ is one of the target clusters with the minimum distance mathematically expressed as follows:

$$\begin{aligned} &\widehat{\mathbf{C}}_i \in (\mathbf{C}_1, \cdots, \mathbf{C}_{i-1}, \mathbf{C}_{i+1}, \cdots, \mathbf{C}_c), \\ &\text{s.t. } D(\mathbf{C}_i, \widehat{\mathbf{C}}_i) = \min(D(\mathbf{C}_i, \mathbf{C}_1), \cdots, D(\mathbf{C}_i, \mathbf{C}_{i-1}), D(\mathbf{C}_i, \mathbf{C}_{i+1}), \cdots, D(\mathbf{C}_i, \mathbf{C}_c)) \end{aligned} \tag{9}$$

Having considered all reference clusters, their nearest clusters $\{\widehat{\mathbf{C}}_1,\cdots,\widehat{\mathbf{C}}_c\}$ are used in anomaly detection instead of $\{\mathbf{C}_1,\ldots,\mathbf{C}_c\}$. In contrast to most of the cluster-based anomaly detectors, the NCS does not allow the information of all clusters to use in the process of anomaly detection. Moreover, it is possible that a target segment is selected as the nearest cluster of some reference segments. For these reasons, the NCS can ignore those features that are influenced by any variability condition so that this benefit enables it to mitigate the negative effects of the E/O variability.

3.4. Anomaly detection by locally robust Mahalanobis-squared distance

Anomaly detection via the LRMSD metric is carried out in two main parts. *First*, the outputs of the NCS (i.e., the nearest clusters) are incorporated into the distance function instead of the mean vector of the whole training data. *Second*, the fast algorithm of the minimum covariance determinant (MCD) proposed by Rousseeuw and Driessen [38], called here FAST-MCD, is considered to estimate the robust version of the covariance matrix of each nearest cluster. Given the matrix of the modal frequencies $\mathbf{X}\in\mathbb{R}^{p\times n}$ (i.e., the whole training data), the FAST-MCD selects h samples out of n, where $\frac{n}{2} < h \leq n$, whose classical covariance matrix has the lowest possible determinant. Accordingly, FAST-MCD gives a robust covariance matrix of the h selected samples [38].

Using the nearest clusters and their robust covariance matrices, it suffices to replace the training and test feature samples in the LRMSD equation and determine their anomaly scores. Given the i^{th} training feature sample $\mathbf{x}_i$, its LRMSD value or damage index (DI) is computed as follows:

$$DI(\mathbf{x}_i) = \min\left(\sum_{t=1}^{r_j} \left(\left(\mathbf{x}_i - \widehat{\mathbf{c}}_j^{(t)} \right)^T \widehat{\mathbf{H}}_j^{-1} \left(\mathbf{x}_i - \widehat{\mathbf{c}}_j^{(t)} \right) \right) \right) \tag{10}$$

where $i=1,\ldots,n$; $\widehat{\mathbf{c}}_j^{(t)} \in \mathbb{R}^p$ is the t^{th} column vector of the j^{th} nearest cluster $\widehat{\mathbf{C}}_j$, where $t=1,\ldots,r_j$ and $j=1,\ldots,c$; and $\widehat{\mathbf{H}}_j \in \mathbb{R}^{p\times p}$ denotes the robust covariance matrix of this cluster. Having considered the c nearest clusters, one can determine c cumulative LRMSD values and subsequently adopt the minimum quantity as the final anomaly score of $\mathbf{x}_i$. For all training samples, it can be obtained n distance quantities $\{DI(\mathbf{x}_1),\ldots,DI(\mathbf{x}_n)\}$. To make a reliable decision, it needs to estimate a threshold limit via the obtained distances. Using the standard confidence interval under a significance level (α), the threshold limit is estimated in the following form:

$$\tau = \mu_{DI} + \zeta_\alpha \sigma_{DI} \tag{11}$$

where μ_{DI} and σ_{DI} represent the mean and standard deviation of the novelty scores $\{DI(\mathbf{x}_1),\ldots,DI(\mathbf{x}_n)\}$. Moreover, ζ_α refers to the $1\text{–}\alpha$ critical value of the distribution of these scores.

In the inspection phase, if all test features are collected sequentially,

one can generate the test matrix $\mathbf{Z}\in\mathbb{R}^{p\times m}$, where m stands for the number of test samples. By incorporating the l^{th} test sample $\mathbf{z}_l$, where l=1,2,…,m, the process of anomaly detection is performed by using the nearest clusters $\{\widehat{\mathbf{C}}_1,\cdots,\widehat{\mathbf{C}}_c\}$ and their robust covariance matrices $\{\widehat{\mathbf{H}}_1,\cdots,\widehat{\mathbf{H}}_c\}$. Accordingly, it only suffices to replace $\mathbf{z}_l$ with $\mathbf{x}_i$ in Eq. (10) and obtain its anomaly score $DI(\mathbf{z}_l)$. For the assessment of the state of the structure, if the anomaly score of the test sample exceeds the threshold (i.e., $DI(\mathbf{z}_l) > \tau$), the proposed UML method triggers the occurrence of damage. This means that the structure sustained from damage. In contrast, if the anomaly score is smaller than the threshold, it makes sense of the undamaged state of the structure.

4. Validation by real-world bridge structures

4.1. A concrete box-girder bridge

This structure was a three-span pretensioned concrete box-girder bridge, called the Z24 Bridge, which was constructed in Switzerland between 1961 and 1963 [39]. The dimensions of this bridge included the main span of 30 m and two sides of 14 m. Fig. 3 displays the Z24 Bridge, its side and top views, and some actual images. The bridge superstructure was comprised of a two-cell box girder and tendons in the three webs. The two abutments contained triple concrete columns connected with concrete hinges to the girder, while the two intermediate supports were concrete piers clamped into the girder. Even though the Z24 Bridge operated normally, it was demolished in 1998 to construct a new bridge with a larger side span. Before this procedure, the bridge was subjected to several progressive damage patterns under a long-term continuous monitoring test. This test was carried out during one year before demolition in an effort to quantify the environmental variability of the bridge dynamics, while the progressive damage patterns were imposed over a month, shortly before complete demolition [39].

During the monitoring program, an operational modal analysis (OMA) based on stochastic subspace identification was conducted by Peeters and De Roeck [13] to identify long-term modal properties from acceleration time histories. In this article, the natural frequencies of four modes are considered to assess the proposed method. The total number of measured natural frequencies related to both the undamaged and damaged conditions is identical to 5652. Based on the proposed initial data analysis, the missing values are removed from the modal dataset, in which case the numbers of missing samples for the first, second, third, and fourth modes correspond to 101, 375, 240, and 1294, respectively. Hence, the final collection of the natural frequencies contains 3932 feature samples, where the first 3475 samples pertain to the undamaged state and the remaining 457 samples are associated with the damaged condition. Fig. 4 illustrates the final natural frequencies (i.e., the clean features) of the Z24 Bridge, where the acronyms "E/O", "NC", and "DC" refer to Environmental/Operational, Normal (undamaged) Condition, and Damaged Condition, respectively. As can be seen, the natural frequencies of the NC were seriously influenced by the E/O conditions, which cause sudden and sharp increases. For this reason, the proposed method is suggested to deal with this issue.

To perform the proposed method, it needs to define the training and test data. In this regard, 75% of the natural frequencies of the NC is gathered to generate the training matrix $\mathbf{X}\in\mathbb{R}_{4\times 2606}$, which includes 2606 feature vectors (n) from four modes (p). Furthermore, the remaining 25% of the natural frequencies of the NC as well as all features of the DC are collected to make the test matrix $\mathbf{Z}\in\mathbb{R}_{4\times 1326}$, where the number 1326 refers to the total number of test samples (m). It should be mentioned that the first 869 feature vectors (i.e., the natural frequencies related to the samples 2607–3475) of the test matrix are equivalent to the validation data.

Having considered the training matrix, the second step of the proposed method begins by segmenting $\mathbf{X}$ into c clusters via the spectral clustering. For this purpose, one needs to determine the optimal cluster number by the gap statistic under some sample clusters. Fig. 5 shows the values of the gap statistic (G) by considering 29 sample clusters (i.e., it starts with 2 and ends with 30). As can be seen, the optimal cluster number by satisfying Eq. (7) coincides with the 13$^{\text{th}}$ sample, which means that c=13. Hence, the training matrix is divided into 13 segments $\{\mathbf{C}_1,\ldots,\mathbf{C}_{13}\}$. Fig. 6 illustrates the cluster labels for all training samples and the number of samples of each cluster. According to the proposed NCS technique, the next step of the proposed method is to find the nearest cluster of each segment and use it as the representative of that cluster in anomaly detection. The labels of the nearest clusters of all 13 segments are shown in Fig. 7(a). For example, the nearest cluster of the first segment is $\widehat{\mathbf{C}}_1=\mathbf{C}_8$. In addition, Fig. 7(b) displays the amounts of the CMSD between $\mathbf{C}_1$ and the target clusters $\{\mathbf{C}_2,\ldots,\mathbf{C}_{13}\}$. As can be observed, the eighth cluster makes the smallest distance with the first cluster, in which case $\mathbf{C}_8$ is the representative of $\mathbf{C}_1$ in anomaly

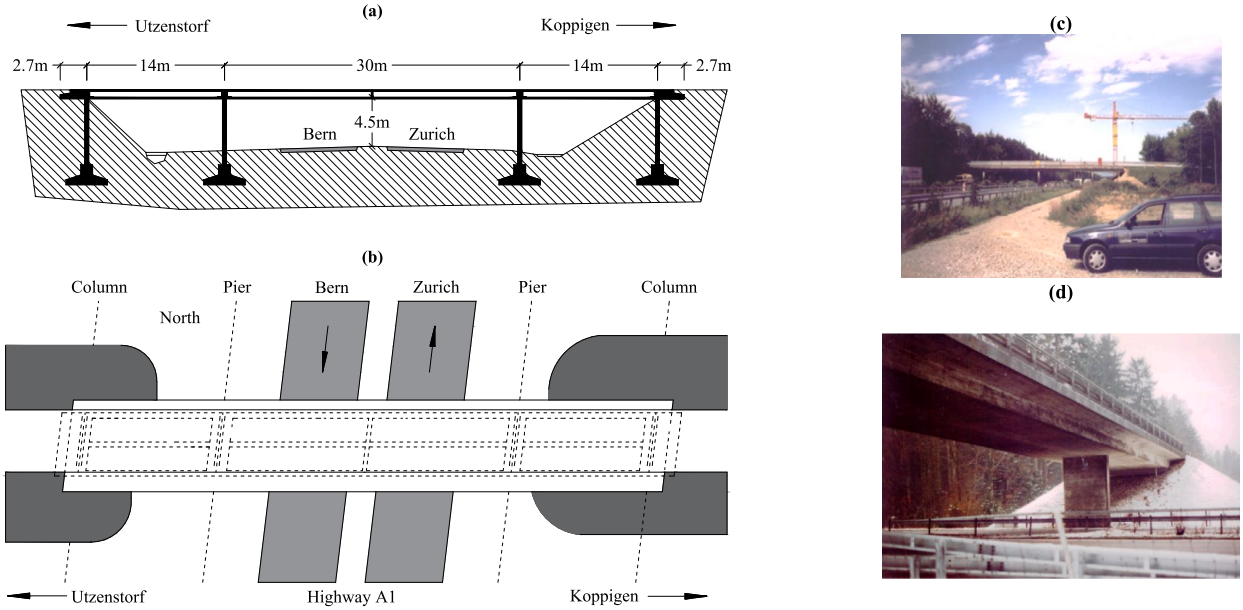

Fig. 3. The Z24 Bridge: (a) the side view and the key dimensions [13], (b) the top view [13], (c) the image of the bridge side view [40], (d) the image of one of the piers and deck [41].

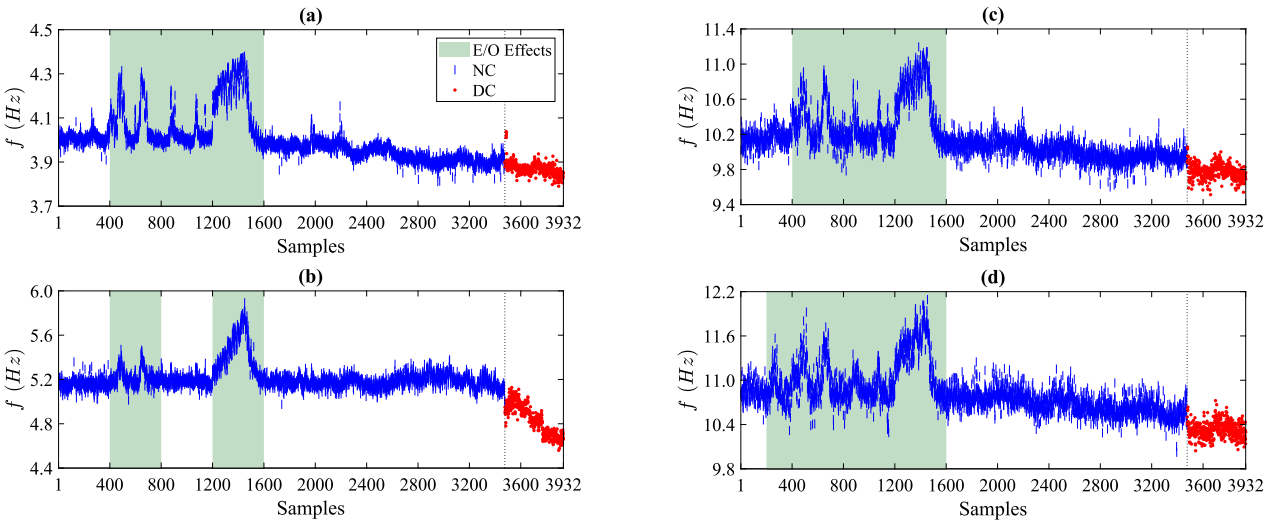

Fig. 4. The final natural frequencies (clean features) of the Z24 Bridge: (a) Mode 1, (b) Mode 2, (c) Mode 3, (d) Mode 4.

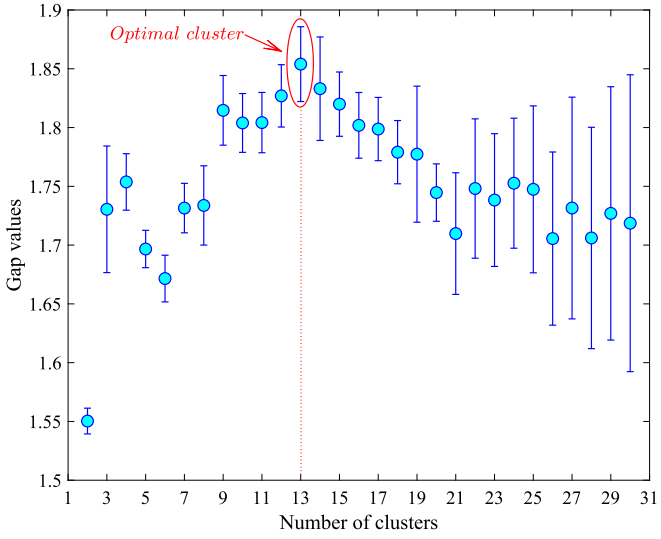

Fig. 5. Selection of the optimal cluster number concerning the spectral clustering by the gap statistic concerning the Z24 Bridge.

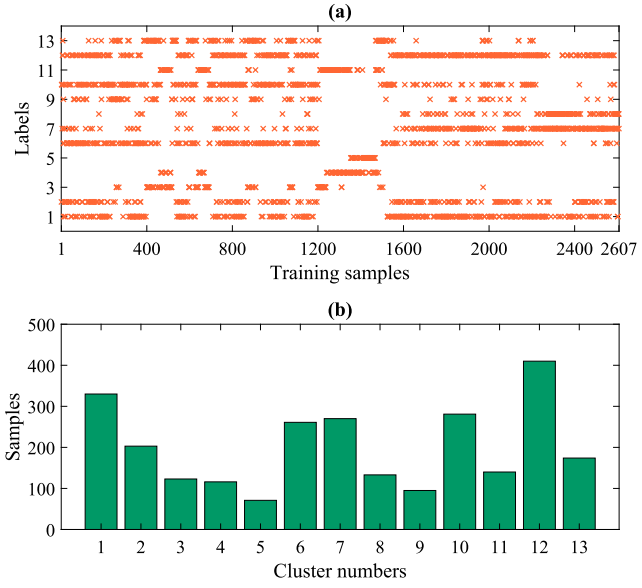

Fig. 6. The outputs of the data segmentation concerning the Z24 Bridge: (a) the cluster labels regarding all training points, (b) the number of samples within each cluster.

detection.

Once all nearest clusters $\{\widehat{\mathbf{C}}_1, \cdots, \widehat{\mathbf{C}}_{13}\}$ have been selected, the clustered features within these segments are applied to estimate their robust covariance matrices $\{\widehat{\mathbf{H}}_1, \cdots, \widehat{\mathbf{H}}_{13}\}$. Finally, the last step of the proposed method utilizes the selected nearest clusters, the robust covariance matrices, and all training and test samples to compute the LRMSD values $\{DI(\mathbf{x}_1),\ldots,DI(\mathbf{x}_{2606})\}$ and $\{DI(\mathbf{z}_1),\ldots,DI(\mathbf{z}_{1326})\}$. Under the significance level α=0.001 (i.e., ζ_α=3.2905), a decision threshold is estimated by applying the anomaly scores of the training points. It needs to clarify that because the proposed UML method has been proposed to mitigate the variability condition and provide smooth and discriminative anomaly scores, one can choose a small rate of significance level.

By accumulating the distance quantities of the training and test data points and comparing them with the decision threshold, Fig. 8 illustrates the result of anomaly detection in the Z24 Bridge. As can be seen, the majority of the DI values of the training and validation points are inserted below the threshold line with the exception of some false positive errors. An important observation in Fig. 8 is that the unexpected sharp increases in the natural frequencies concerning the samples 400–1600 are no longer present in the anomaly indices of the NC. This demonstrates the positive influence of the proposed UML method and also the NCS algorithm to handle the E/O effects. Alternatively, most of the DI values of the DC exceed the threshold except for the only one point. Without considering the threshold limit, one can discern that there is a clear difference between the anomaly scores of the NC and DC. This conclusion demonstrates high damage detectability obtained by the proposed method.

Despite such a reliable and effective result under severe E/O conditions, it is important to compare the proposed method with its counterparts. The comparative studies are based on evaluating the SHM result via a parametric clustering-based anomaly detector and a non-parametric distance-based anomaly detector. The first approach relies

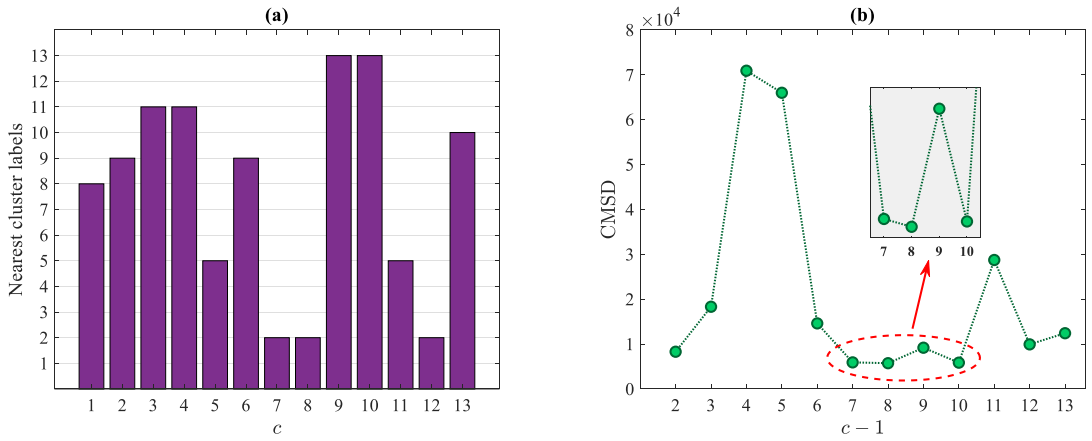

Fig. 7. The outputs of the NCS concerning the Z24 Bridge: (a) the labels of the nearest clusters of 13 segments, (b) the CMSD values between the first cluster and its target clusters.

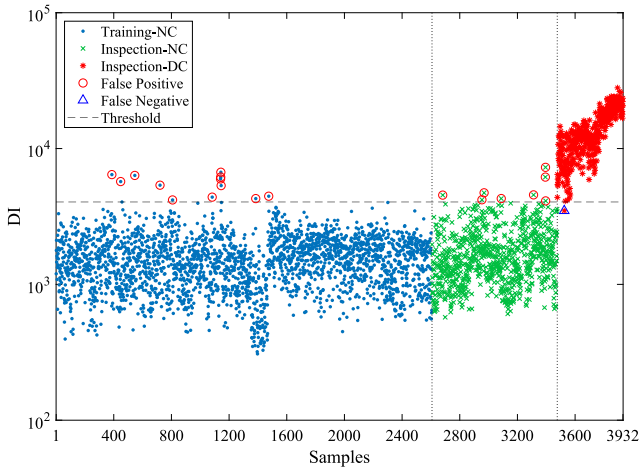

Fig. 8. Anomaly detection in the Z24 Bridge by the proposed UML method.

Table 1
Performance evaluation of the proposed UML and classical methods in the SHM problem of the Z24 Bridge.

Methods	Triple decision-making errors		
	False positive	False negative	Misclassification
UML	20 (0.57 %)	1 (0.21 %)	21 (0.53 %)
SC-MSD	135 (3.88 %)	0 (0.00 %)	135 (3.43 %)
MSD	53 (1.52 %)	280 (61.04 %)	333 (8.46 %)

on the combination of the spectral clustering and the well-known MSD metric. In other words, this technique called here SC-MSD aims to initially cluster the training data into some clusters/segments to provide the main requirements of the MSD; that is, the mean vectors and covariance matrices. Finally, the training and test samples are applied to the MSD to compute their minimum distance values among all clusters. Similar to the proposed UML method, the SC-MSD technique presents a locally parametric anomaly detector, for which the optimal number of clusters needed for the spectral clustering is gained by the gap statistic. The second approach is based on the well-known MSD measure [42], which develops a globally non-parametric anomaly detector. For this approach, one needs to estimate the mean vector and covariance matrix of the whole training data. The comparative studies are conducted to assess the performances of the proposed and classical methods in terms of: (i) the decision-making errors (i.e., false positive, false negative, and misclassification) using a single threshold estimator, and (ii) damage detectability without any threshold.

For the first comparative study, Table 1 lists the numbers and percentages of the triple decision-making errors using the threshold estimator, Eq. (11), based on the significance level equal to α=0.001. Note that the same significance level is considered here to provide a fair comparison. Regarding the false positive error, the proposed method yields the best performance. In contrast, the worst performance belongs to the SC-MSD. On the other hand, both the UML and SC-MSD roughly have the similar false negative errors. Moreover, the MSD-based anomaly detector has the worst performance with the largest false negative error. Finally, the proposed UML method outperforms the SC-MSD and MSD concerning the misclassification (total) error.

For the second comparative study, Fig. 9 shows the DI values of the training and test samples associated with the proposed UML method and the SC-MSD and MSD techniques. Notice that Fig. 9(a) is exactly Fig. 8 without the threshold line. As Fig. 9(a) appears, the UML could effectively eliminate the E/O effects, particularly in the NC, and provide discriminative anomaly scores so that it is simply possible to distinguish the DC from the NC implying high damage detectability of this method. Fig. 9(b) depicts the anomaly scores of the SC-MSD, where there is still a small jump caused by the E/O changes in the DI values of the training data between the samples 1200–1600. Moreover, some increases in the DI values of the validation data are observable. Fig. 9(c) shows the damage indices related to the MSD. As can be seen, a large and sharp increase in the DI quantities concerning the training samples verifies the serious impact of the E/O changes on this technique. On the other hand, the majority of the anomaly scores of the DC are in the same range of the corresponding scores of the NC implying low damage detectability. Thus, it can be concluded that the proposed UML method is clearly better than the SC-MSD and MSD associated with yielding discriminative anomaly scores with the minimum decision-making errors and providing high damage detectability. Furthermore, one can deduce that the local anomaly detectors (e.g., UML and SC-MSD) outperform the global detector (e.g., MSD).

4.2. A steel arch bridge

This structure is a railway steel arch bridge called the KW51 Bridge that connects between Leuven and Brussels in Belgium via the railway line L36N [43]. The KW51 Bridge consists of the total length of 115 m and the width of 12.4 m. Fig. 10 shows the side and top views of the

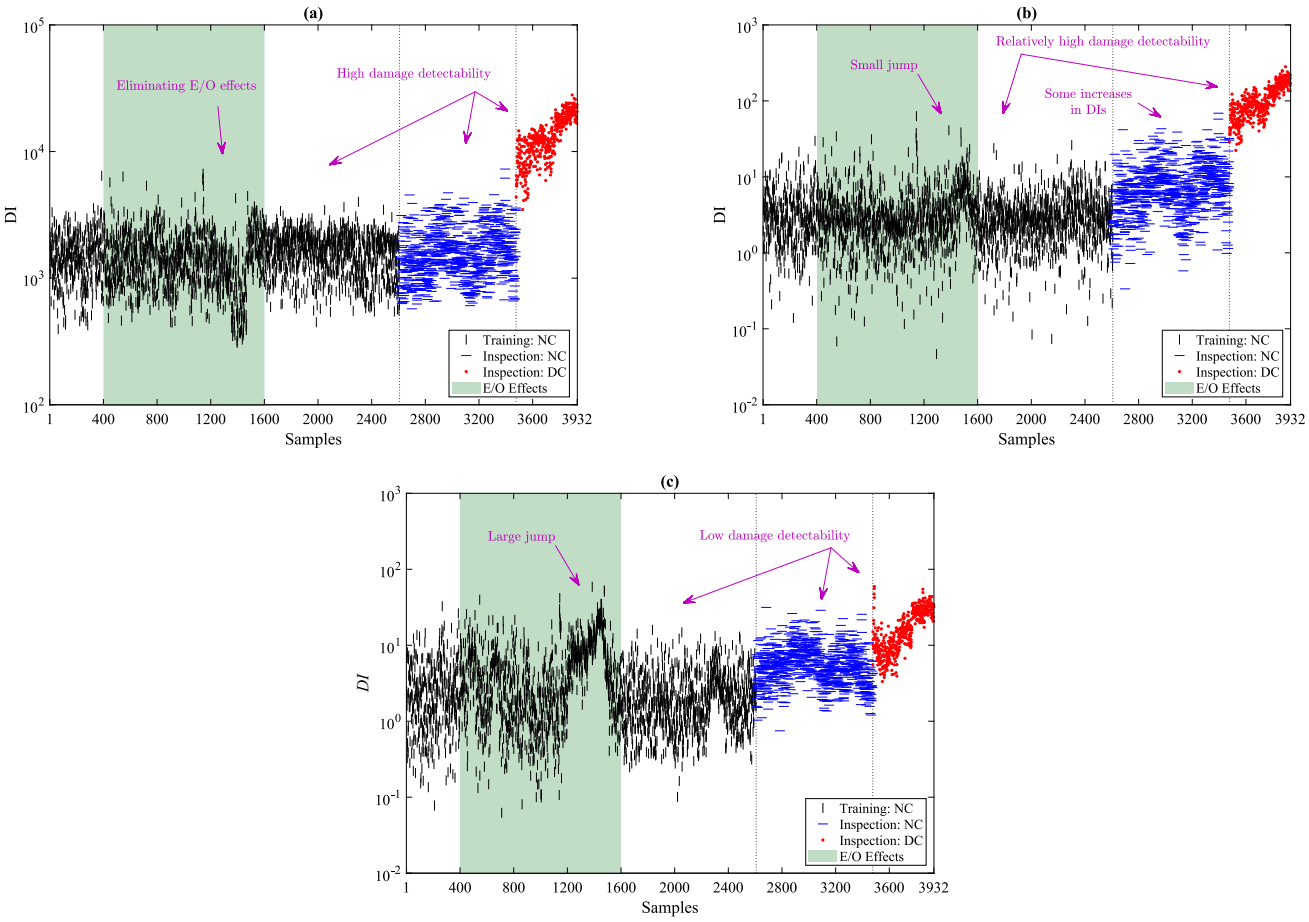

Fig. 9. Performance evaluation in terms of damage detectability concerning the Z24 Bridge: (a) UML, (b) SC-MSD, (c) MSD.

KW51 Bridge as well as its actual images. This structure was strengthened to cope with a construction problem during inspection between 15 May to 27 September 2019. The retrofitting process included strengthening the connections of the diagonals to the arches and the bridge deck [14]. Due to the installation of an SHM system, some vibration responses along with modal properties were released to help researchers to validate their proposed methods [43]. Until now, the KW51 Bridge was incorporated into different SHM applications such as data normalization for removing the effect of environmental variability [14], continuous monitoring by modal frequencies and stain mode shapes under temperature variations and retrofitting [44], OMA [45], and anomaly (damage) detection [34].

An automatic OMA was implemented by Maes and Lombaert [43] to identify modal properties of the KW51 Bridge such as the natural frequencies, mode shapes, and damping ratios between 02 October 2018 to 15 May 2019 (before the retrofit), 16 May 2019 to 26 September 2019 (during the retrofit), and 27 September 2019 and 01 January 2020 (after the retrofit). In the OMA, the acceleration responses corresponding to a period of five minutes of ambient vibration (i.e., no train passages on the bridge) were processed by a reference-based covariance-driven stochastic subspace identification algorithm [14]. Totally, the automated OMA gave 14 modes over time. Accordingly, it can be defined two types

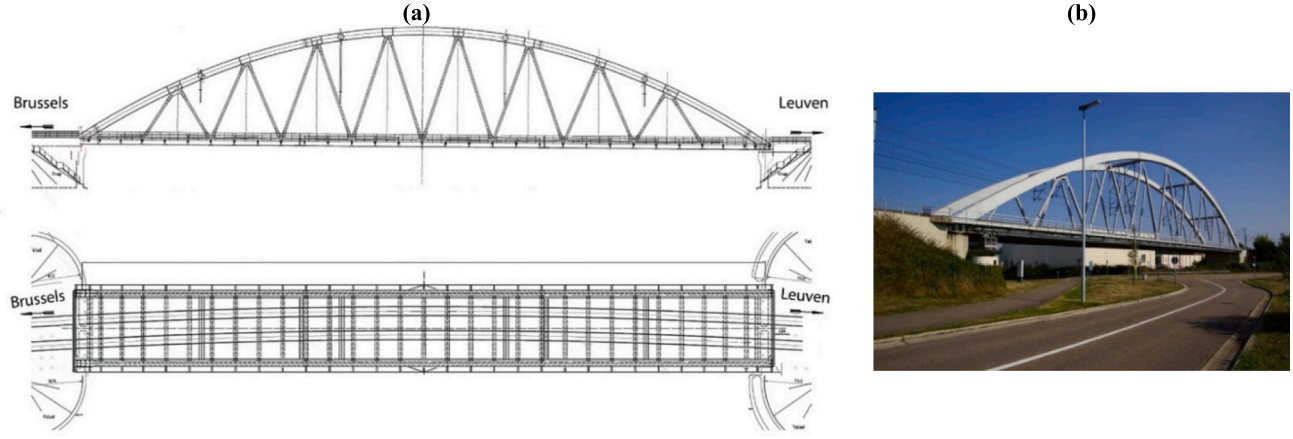

Fig. 10. The KW51 Bridge: (a) the side and top views [14], (b) an image of the south side [45].

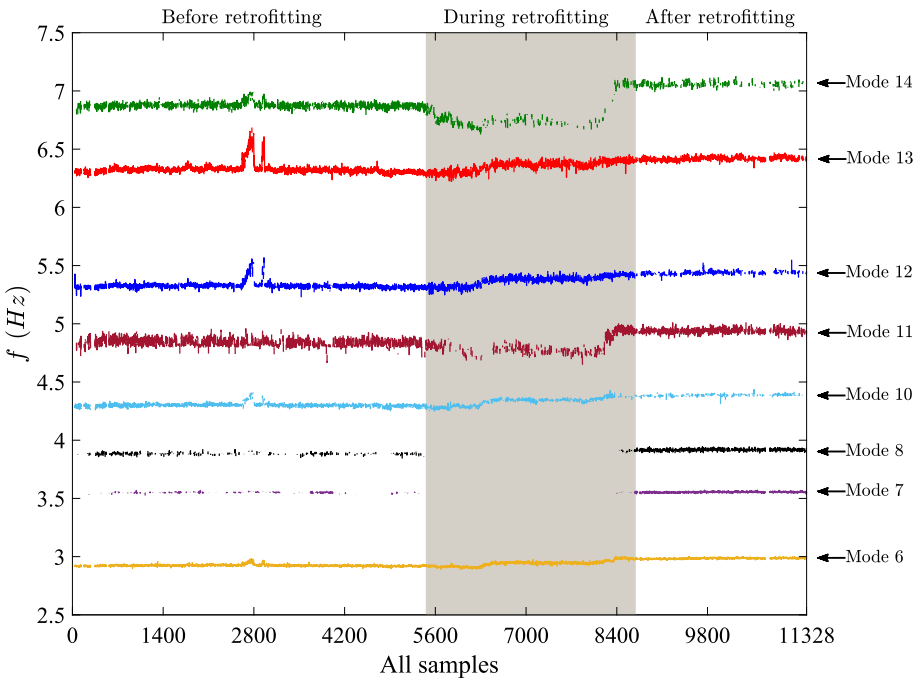

Fig. 11. The complete set of the natural frequencies of the KW51 Bridge concerning the modes 6–8 and 10–14.

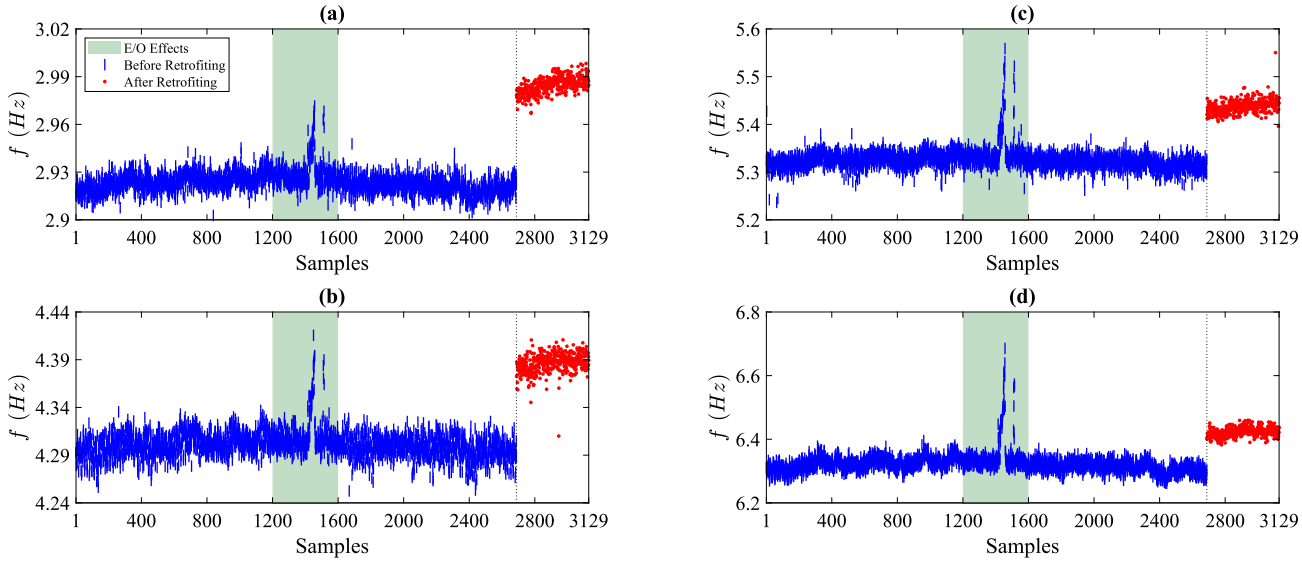

Fig. 12. The final natural frequencies (clean features) of the KW51 Bridge: (a) Mode 6, (b) Mode 10, (c) Mode 12, (d) Mode 13.

of modal datasets based on the variations in the natural frequencies. In the modes 6–8 and 10–14, the retrofit increased the magnitudes of the modal frequencies, while this process decreased such features in the modes 1–5 and 9. In this article, the first group of the natural frequencies is considered to validate the proposed method. Fig. 11 illustrates these modal frequencies before, during, and after retrofitting. Among these modes, some of them consist of numerous missing values that can make obstacles to use in any ML-based SHM due to providing insufficient training data. Based on the initial data analysis, the numbers of missing data among all 11,328 samples correspond to 393, 7963, 8223, 5263, 5111, 3642, 1606, and 6479 for the modes 6–8 and 10–14, respectively. Therefore, the final choice is to incorporate the vertical modes 6, 10, 12, and 13, where the environmental variability (i.e., the sudden sharp increases) seriously affected them. Inspired by Maes et al. [14], the natural frequencies of the bridge before and after retrofitting are used as the dynamic features of the NC and DC, respectively.

After eliminating all missing values, the total number of natural frequencies before and after retrofitting is equal to 3129 as shown in Fig. 12, where the modal frequencies of the samples 1-2688 and 2689-3129 are related to the NC (i.e., before retrofitting) and DC (i.e., after retrofitting), respectively. As this figure reveals, there are sudden and sharp increases in the natural frequencies of the NC between the samples 1200-1600 (i.e., the areas of the E/O effects). This variability pertains to the influence of the ambient temperature around or below 0°C on the modal frequencies, similar to the Z24 Bridge [14]. This conclusion properly verifies the profound effects of the E/O changes on the natural frequencies of civil structures regardless of their material properties. The other important note is that the level of the E/O effects differs between the selected modes. To put it another way, the magnitudes of the natural frequencies of the modes 10, 12, and 13 regarding the samples 1200-

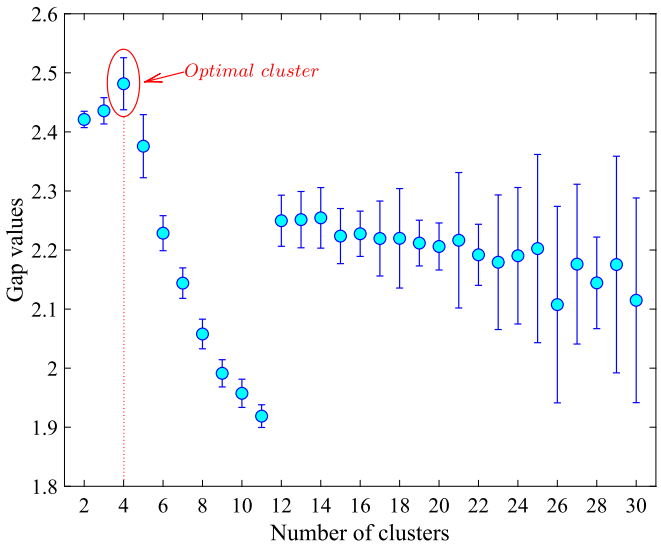

Fig. 13. Selection of the optimal cluster number of the spectral clustering by the gap statistic concerning the KW51 Bridge.

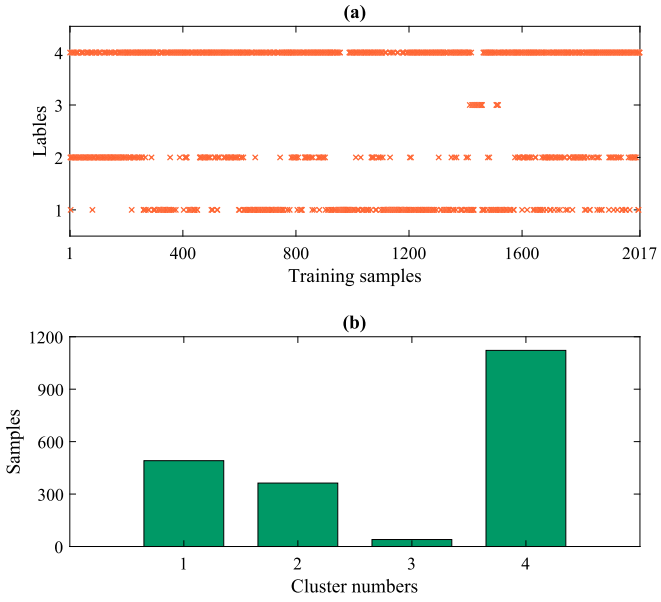

Fig. 14. The outputs of the data segmentation concerning the KW51 Bridge: (a) the cluster labels regarding all training points, (b) the number of samples of each cluster.

1600 are greater in comparison with the corresponding magnitudes related to the DC. This note confirms the strong impact of the environmental variability on the natural frequencies so that the structural changes attributable to the bridge strengthening cannot make such variations. Therefore, similar to the Z24 Bridge, it is attempted to achieve two purposes: (i) removal of the E/O influences, and (ii) accurate discrimination of the simulated DC from the NC.

In a similar manner to the preceding structure, 75% of the natural frequencies of the NC is utilized to construct the training matrix $\mathbf{X}\in\mathbb{R}_{4\times 2016}$ containing 2016 feature vectors (n) of four modes (p). On the other hand, the test matrix $\mathbf{Z}\in\mathbb{R}_{4\times 1113}$ contains 672 samples of the natural frequencies of the NC (i.e., the remaining 25% of the features, which serve as the validation data) and 441 samples of the natural frequencies of the simulated DC. Using the training samples and the gap statistic, Fig. 13 shows the optimal cluster number needed for the step of data segmentation via the spectral clustering under 30 cluster samples. As can be seen, the fourth cluster could meet the condition of Eq. (7), which means that c=4. In this regard, the cluster labels for all training samples and the number of samples within each cluster are illustrated in Fig. 14.

Regarding the third step of the proposed UML method, Fig. 15(a) displays the labels of the nearest clusters of $\{\mathbf{C}_1,\ldots,\mathbf{C}_4\}$, which correspond to $\widehat{\mathbf{C}}_1=\mathbf{C}_3$, $\widehat{\mathbf{C}}_2=\mathbf{C}_3$, $\widehat{\mathbf{C}}_3=\mathbf{C}_2$, and $\widehat{\mathbf{C}}_4=\mathbf{C}_2$. For more details, Fig. 15 (b) presents the CMSD values between $\mathbf{C}_1$ and the target clusters $\{\mathbf{C}_2, \mathbf{C}_3, \mathbf{C}_4\}$. As can be observed, the third cluster produces the smallest distance, which means that $\mathbf{C}_3$ is the representative of $\mathbf{C}_1$ in the process of anomaly detection. Having considered the nearest clusters $\{\widehat{\mathbf{C}}_1, \cdots, \widehat{\mathbf{C}}_4\}$, the selected features within these segments are incorporated to estimate four robust covariance matrices. Accordingly, the nearest clusters and estimated covariance matrices are the main elements of the LRMSD-based novelty detector. Using all training and test samples, their LRMSD values $\{DI(\mathbf{x}_1),\ldots,DI(\mathbf{x}_{2016})\}$ and $\{DI(\mathbf{z}_1),\ldots,DI(\mathbf{z}_{1113})\}$ are computed as the anomaly scores for decision-making. The result of anomaly detection in the KW51 Bridge is displayed in Fig. 16, where the horizontal line refers to the threshold limit obtained from the same threshold estimator and significance level as the Z24 Bridge. It is obvious that most of the DI values of the training and validation points are under the threshold with the exception of a few points. A prominent conclusion is that the sharp increase in the natural frequencies between the samples 1200–1600 is not present in the anomaly scores gained by the proposed method. This verifies the great capability of the UML to mitigate the E/O effects. On the other hand, all of the DI values of the DC are over the threshold indicating the accurate detection of the simulated damage. Regardless of the threshold, it is discerned that there is a clear discrepancy between the anomaly scores of the NC and DC implying high damage detectability of the proposed UML method.

To further validate the superiority of UML over the classical

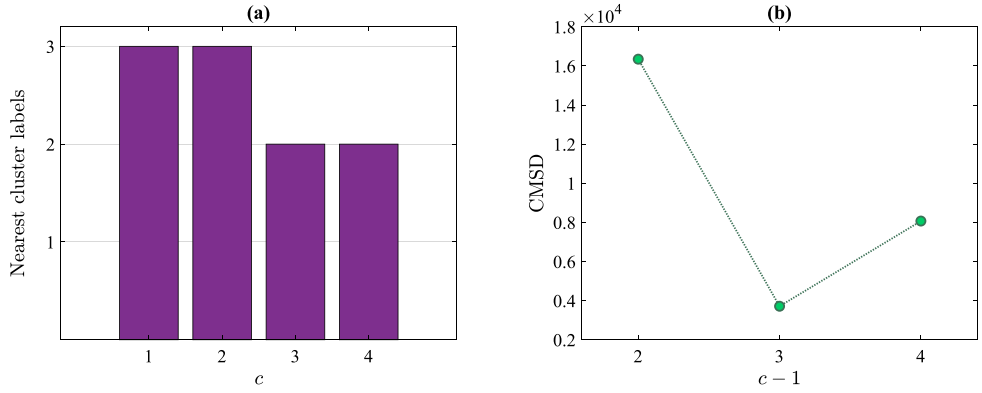

Fig. 15. The outputs of the NCS concerning the KW51 Bridge: (a) the labels of the nearest clusters of all four segments, (b) the CMSD values between the first cluster and its target clusters.

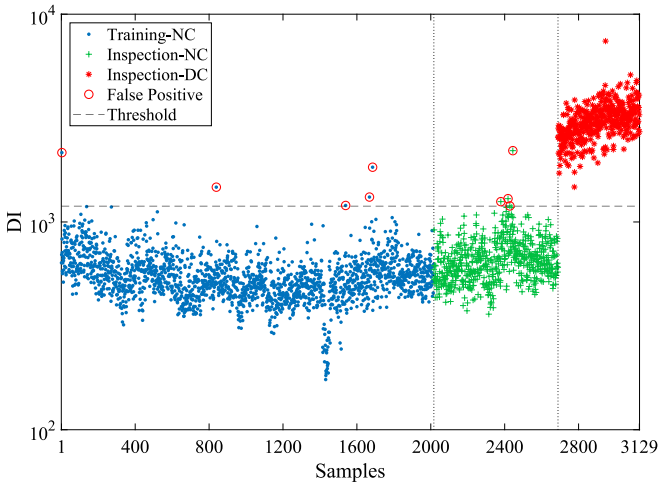

Fig. 16. Anomaly detection in the KW51 Bridge by the proposed UML method.

Table 2
Performance evaluation of the proposed UML and classical methods in the SHM problem of the KW51 Bridge.

Methods	Triple decision-making errors		
	False positive	False negative	Misclassification
UML	9 (0.33 %)	0 (0.00 %)	9 (0.28 %)
SC-MSD	41 (1.52 %)	0 (0.00 %)	41 (1.31 %)
MSD	24 (0.89 %)	0 (0.00 %)	24 (0.76 %)

techniques SC-MSD and MSD, Table 2 presents the numbers and percentages of the triple decision-making errors in the SHM procedure of the KW51 Bridge. As the data in this table indicates, the proposed UML method gives the best performance in all error cases. Although all three techniques do not have any false negative error, one can realize that the proposed method outperforms the SC-MSD and MSD regarding the false positive and misclassification errors. Such outputs resemble the conclusions regarding the Z24 Bridge. In relation to the false negative error in Table 2, it should be clarified that the main reason for such output pertains to the difference between the magnitudes of the modal frequencies of the NC and DC. According to the assumption regarding the simulated DC (i.e., the bridge after retrofitting), one can observe in the modal frequencies of this condition (see Fig. 12) that there is a relatively large difference between the modal frequencies of the NC and DC. This property also affects the proposed method, in which case no false negative error occurred in the SHM process.

Furthermore, Fig. 17 compares the UML, SC-MSD, and MSD methods for the problem of damage detectability without any threshold. In Fig. 17(a) and (b), one can perceive that the local unsupervised anomaly detectors (i.e., UML and SC-MSD) could appropriately deal with the E/O effects. Nonetheless, the poor performance of SC-MSD relates to its low damage detectability compared to UML. From Fig. 17(b), it can be realized that the DI values of the simulated DC are in the vicinity of the corresponding scores of the NC. Regarding the classical MSD technique, it is simply observed that this approach could not cope with the major challenge of the E/O effects and the sharp increase is still existence in the DI values of the NC. Since the scales of some DI values between the samples 1200–1600 are equal to or greater than some DI values of the simulated DC, one can conclude that MSD could not provide high damage detectability.

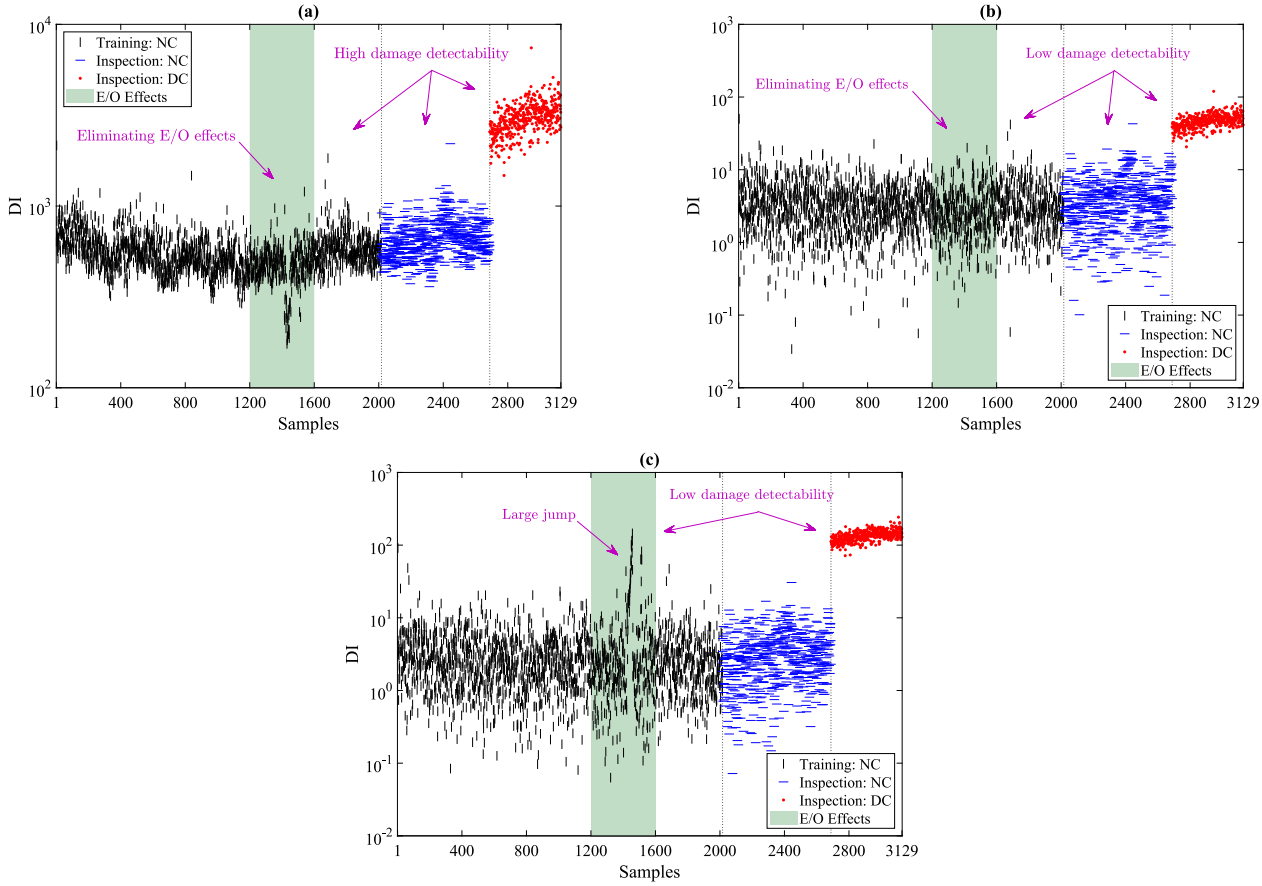

Fig. 17. Performance evaluation in terms of damage detectability concerning the KW51 Bridge: (a) UML, (b) SC-MSD, (c) MSD.

5. Conclusions

This article proposed a novel unsupervised learning method based on the concept of meta-learning for long-term SHM under severe E/O effects. The proposed method consisted of four main parts of an initial data analysis for discarding missing samples, data segmentation via the spectral clustering, a subspace searching algorithm by the proposed NCS approach, and anomaly detection through the LRMSD metric. The large sets of the long-term natural frequencies of the concrete (Z24) and steel (KW51) bridges were used to demonstrate the correctness and good performance of the proposed method alongside some comparative studies.

The results of this article indicated that the proposed UML method is clearly able to remove the E/O effects (i.e., the sharp increases in the natural frequencies caused by freezing temperature conditions) and provide discriminative anomaly scores for accurate damage detection. Furthermore, this conclusion verifies the idea of the proposed NCS approach. The initial data analysis can help us to disregard missing values and provide homogeneous real training data for the learning process. The comparative studies revealed that the proposed UML method is superior to the SC-MSD and MSD techniques in terms of yielding fewer errors and higher damage detectability. The comparison results also indicated that the locally unsupervised learning methods such as UML and SC-MSD are much more successful and reliable than the globally unsupervised learning techniques such as MSD.

Despite the reliable and reasonable results of SHM gained by the proposed UML method, some issues should also be considered and addressed in further research. Regarding the problem of missing data, the proposed method disregarded such data. For further research, it is recommended to recover missing samples and implement the SHM procedure by the original and recovered features. The other important issue relates to long-term SHM under the concept of unsupervised learning. For this problem, one needs to measure data and extract features in a fixed period and also assume that the structure is undamaged during this time. Therefore, it is suggested to pay more attention to other ML algorithms such as semi-supervised learning, active learning, and self-supervised learning.

CRediT authorship contribution statement

Alireza Entezami: Conceptualization, Methodology, Software, Writing – original draft, Funding acquisition. **Hassan Sarmadi:** Conceptualization, Methodology, Software, Writing – review & editing, Resources. **Bahareh Behkamal:** Methodology, Writing – review & editing, Validation.

Declaration of Competing Interest

The authors declare that they have no known competing financial interests or personal relationships that could have appeared to influence the work reported in this paper.

Data availability

Data will be made available on request.

Acknowledgement

This research was partially funded by the European Space Agency (ESA) under ESA Contract No. 4000132658/20/NL/MH/ac.

References

[1] He Z, Li W, Salehi H, Zhang H, Zhou H, Jiao P. Integrated structural health monitoring in bridge engineering. Autom Constr 2022;136:104168.
[2] Sivasuriyan A, Vijayan DS, Górski W, Wodzyński Ł, Vaverková MD, Koda E. Practical implementation of structural health monitoring in multi-story buildings. Buildings 2021;11:263.
[3] Sivasuriyan A, Vijayan DS, Munusami R, Devarajan P. Health assessment of dams under various environmental conditions using structural health monitoring techniques: a state-of-art review. Environ Sci Pollut Res 2022;29:86180–91.
[4] Lynch JP, Sohn H, Wang ML. Sensor Technologies for Civil Infrastructures: Volume 2: Applications in Structural Health Monitoring. 2nd ed. Cambridge, MA, United States: Elsevier; 2022.
[5] Salehi H, Burgueño R, Chakrabartty S, Lajnef N, Alavi AH. A comprehensive review of self-powered sensors in civil infrastructure: State-of-the-art and future research trends. Eng Struct 2021;234:111963.
[6] Kita A, Cavalagli N, Ubertini F. Temperature effects on static and dynamic behavior of Consoli Palace in Gubbio. Italy Mech Syst Sig Process 2019;120:180–202.
[7] Ni YQ, Wang YW, Zhang C. A Bayesian approach for condition assessment and damage alarm of bridge expansion joints using long-term structural health monitoring data. Eng Struct 2020;212:110520.
[8] Larsson C, Abdeljaber O, Bolmsvik Å, Dorn M. Long-term analysis of the environmental effects on the global dynamic properties of a hybrid timber-concrete building. Eng Struct 2022;268:114726.
[9] Magalhães F, Cunha Á. Explaining operational modal analysis with data from an arch bridge. Mech Syst Sig Process 2011;25:1431–50.
[10] Zhou Y, Sun L. Effects of environmental and operational actions on the modal frequency variations of a sea-crossing bridge: A periodicity perspective. Mech Syst Sig Process 2019;131:505–23.
[11] Zonno G, Aguilar R, Boroschek R, Lourenço PB. Analysis of the long and short-term effects of temperature and humidity on the structural properties of adobe buildings using continuous monitoring. Eng Struct 2019;196:109299.
[12] Martins N, Caetano E, Diord S, Magalhães F, Cunha Á. Dynamic monitoring of a stadium suspension roof: Wind and temperature influence on modal parameters and structural response. Eng Struct 2014;59:80–94.
[13] Peeters B, De Roeck G. One-year monitoring of the Z24-Bridge: Environmental effects versus damage events. Earthquake Eng Struct Dyn 2001;30:149–71.
[14] Maes K, Van Meerbeeck L, Reynders EPB, Lombaert G. Validation of vibration-based structural health monitoring on retrofitted railway bridge KW51. Mech Syst Sig Process 2022;165:108380.
[15] Wang Z, Yang D-H, Yi T-H, Zhang G-H Han J-G. Eliminating environmental and operational effects on structural modal frequency: A comprehensive review. Struct Contr Health Monit 2022;29:e3073.
[16] Salehi H, Burgueño R. Emerging artificial intelligence methods in structural engineering. Eng Struct 2018;171:170–89.
[17] Zhang Y, Yuen K-V. Review of artificial intelligence-based bridge damage detection. Adv Mech Eng 2022;14(9).
[18] Li Y, Bao T, Chen Z, Gao Z, Shu X, Zhang K. A missing sensor measurement data reconstruction framework powered by multi-task Gaussian process regression for dam structural health monitoring systems. Meas 2021;186:110085.
[19] Sarmadi H, Yuen K-V. Early damage detection by an innovative unsupervised learning method based on kernel null space and peak-over-threshold. Comput Aided Civ Inf 2021;36:1150–67.
[20] Giglioni V, García-Macías E, Venanzi I, Ierimonti L, Ubertini F. The use of receiver operating characteristic curves and precision-versus-recall curves as performance metrics in unsupervised structural damage classification under changing environment. Eng Struct 2021;246:113029.
[21] Mousavi M, Gandomi AH, Abdel Wahab M, Glisic B. Monitoring onsite-temperature prediction error for condition monitoring of civil infrastructures. Struct Contr Health Monit 2022;29:e3112.
[22] Daneshvar MH, Sarmadi H. Unsupervised learning-based damage assessment of full-scale civil structures under long-term and short-term monitoring. Eng Struct 2022;256:114059.
[23] Rogers TJ, Worden K, Fuentes R, Dervilis N, Tygesen UT, Cross EJ. A Bayesian non-parametric clustering approach for semi-supervised Structural Health Monitoring. Mech Syst Sig Process 2019;119:100–19.
[24] Sarmadi H, Yuen K-V. Structural health monitoring by a novel probabilistic machine learning method based on extreme value theory and mixture quantile modeling. Mech Syst Sig Process 2022;173:109049.
[25] Entezami A, Shariatmadar H, De Michele C. Non-parametric empirical machine learning for short-term and long-term structural health monitoring. Struct Health Monit 2022;21:2700–18.
[26] Ma Z, Yun C-B, Wan H-P, Shen Y, Yu F, Luo Y. Probabilistic principal component analysis-based anomaly detection for structures with missing data. Struct Contr Health Monit 2021;28:e2698.
[27] Ma Z, Luo Y, Yun C-B, Wan H-P, Shen Y. An MPPCA-based approach for anomaly detection of structures under multiple operational conditions and missing data. Struct Health Monit 2022.
[28] Xu M, Li J, Wang S, Hao H, Tian H, Han J. Structural damage detection by integrating robust PCA and classical PCA for handling environmental variations and imperfect measurement data. Adv Struct Eng 2022;25:1815–28.
[29] Xu M, Wu W, Li J, Au FTK, Wang S, Hao H, et al. Structural damage detection using low-rank matrix approximation and cointegration analysis. Eng Struct 2022;267:114677.
[30] Soo Lon Wah W, Owen JS, Chen Y-T, Elamin A, Roberts GW. Removal of masking effect for damage detection of structures. Eng Struct 2019;183:646–61.
[31] Sarmadi H, Entezami A, De Michele C. Probabilistic data self-clustering based on semi-parametric extreme value theory for structural health monitoring. Mech Syst Sig Process 2023;187:109976.

[32] Oktar Y, Turkan M. A review of sparsity-based clustering methods. Signal Process 2018;148:20–30.
[33] Suárez JL, García S, Herrera F. A tutorial on distance metric learning: Mathematical foundations, algorithms, experimental analysis, prospects and challenges. Neurocomputing 2021;425:300–22.
[34] Sarmadi H, Entezami A, Behkamal B, De Michele C. Partially online damage detection using long-term modal data under severe environmental effects by unsupervised feature selection and local metric learning. J Civ Struct Health Monit 2022;12:1043–66.
[35] Meta-Learning VJ. In: Automated Machine Learning: Methods, Systems, Challenges. Cham: Springer International Publishing; 2019. p. 35–61.
[36] Von Luxburg U. A tutorial on spectral clustering. Stat Comput 2007;17:395–416.
[37] Tibshirani R, Walther G, Hastie T. Estimating the number of clusters in a data set via the gap statistic. J Roy Stat Soc Ser B (Stat Method) 2001;63:411–23.
[38] Rousseeuw PJ, Driessen KV. A fast algorithm for the minimum covariance determinant estimator. Technometrics 1999;41:212–23.
[39] Reynders E, De Roeck G. Continuous Vibration Monitoring and Progressive Damage Testing on the Z24 Bridge. Encyclopedia of Structural Health Monitoring. Chichester, United Kingdom: John Wiley & Sons, Inc.; 2009.
[40] Maeck J, De Roeck G. Description of Z24 Bridge. Mech Syst Sig Process 2003;17:127–31.
[41] Steenackers G, Guillaume P. Structural health monitoring of the Z24 Bridge in presence of environmental changes using modal analysis. 23rd Proceeding of International Modal Analysis Conference (IMAC): The Society of Experimental Mechanics (SEM); 2005.
[42] Entezami A. Statistical Decision-Making by Distance Measures. Structural Health Monitoring by Time Series Analysis and Statistical Distance Measures. Cham: Springer International Publishing; 2021. p. 59–79.
[43] Maes K, Lombaert G. Monitoring Railway Bridge KW51 Before, During, and After Retrofitting. J Bridge Eng 2021;26:04721001.
[44] Anastasopoulos D, Maes K, De Roeck G, Lombaert G, Reynders EPB. Influence of frost and local stiffness variations on the strain mode shapes of a steel arch bridge. Eng Struct 2022;273:115097.
[45] Anastasopoulos D, De Roeck G, Reynders EPB. One-year operational modal analysis of a steel bridge from high-resolution macrostrain monitoring: Influence of temperature vs. retrofitting. Mech Syst Sig Process 2021;161:107951.
[46] Entezami A, Sarmadi H, De Michele C. Probabilistic damage localization by empirical data analysis and symmetric information measure. Meas 2022;198:111359.